Functional Aerogels

DOI: 10.1002/ange.201305137

Nanocellulose Aerogels Functionalized by Rapid Layer-by-Layer Assembly for High Charge Storage and Beyond**

Mahiar Hamedi, Erdem Karabulut, Andrew Marais, Anna Herland, Gustav Nyström, and Lars Wågberg*

Aerogels are solid materials with desirable properties, including very low densities, thermal conductivities, and high specific surface areas. These properties offer numerous possibilities for aerogels as functional materials. A number of mesoscopic materials have been used as building blocks for aerogels, including carbon nanotubes[1] and graphene.[2] The true potential of aerogels may be realized when functional materials are added to achieve more advanced usability. Some examples include the demonstration of oxygen-reduction reactions in graphene aerogels,[3] mechanoresponsive nanocellulose aerogels,[4] and magnetic aerogels.[5] In these examples, the active aerogels were designed from the bottom up for each specific application. However the bottom-up approach presents challenges and shortcomings, including:

- The necessity of adding the active materials to the aerogel building block prior to making the aerogel. This may demand complex chemistry, and the functional materials may not be compatible with the building-block dispersion or the aerogel process.
- The inability to control the thickness of the active material at the nanoscale, and the inability to construct multiple layers of different materials.
- The need to design completely new aerogel building blocks and preparation procedures for each desired function.

Layer by layer (LbL) assembly is a generic technique for coating functional materials onto surfaces,[6] and a large number of applications based on this technique have been accomplished.[7] It is therefore easy to envision a diversity of advanced materials that can be made using the LbL method for the self-assembly of functional materials onto aerogels. However, no aerogel material suitable for LbL and no feasible method for the LbL assembly onto aerogels have been found to date. Examples of LbL assemblies onto porous structures include the nanotube-assembly on macroporous carbon paper,[8] fire-resistant three-layer structures on a polyurethane foam,[9] and an LbL nanosheath on a polymer-blend porous structure.[10]

Herein, we report a robust and rapid method for the LbL assembly of functional polymers and nanoparticles on cross-linked nanocellulose aerogels with a porosity close to 99%, high strength, and nanoscale shape integrity in water. We show that the LbL assembly of thin films of biomolecules, conducting polymers, and carbon nanotubes can be used for adding electronic and mechanical properties. Furthermore, we demonstrate that aerogels with dry-strength and elastic wet strength enhancement, elastic mechanoresponsive resistance, and supercapacitor properties with specific capacitance values exceeding 400 $F g^{-1}$ have been developed.

In this study, we have chosen to work with nanofibrillated cellulose (NFC) as the aerogel building block. NFC is a rapidly emerging class of bio-friendly bulk nanomaterial that offers tremendous possibilities for the aqueous self-assembly of a range of advanced micro- and nano-structures.[11] By blending functional materials in NFC dispersions, active composites have also been developed, such as magnetic nanopaper[5] and carbon nanotubes.[4] Aside from nanostructuring, the high anionic or cationic surface charge of NFCs also presents possibilities for non-covalent, yet strong ionic interactions. The most intriguing implication is the possibility to use the LbL assembly method on NFC structures. It has been demonstrated that well-defined LbL structures can be formed by combining NFC and different types of cationic polyelectrolytes.[12]

NFC-based aerogels should therefore also be ideal candidates for LbL assembly. However, as NFC is dispersible in water, the aerogel nanostructure will fully disintegrate during an LbL assembly. It has recently been demonstrated that covalent cross-linking of NFC aerogels[13] results in macroscale shape recovery of NFC aerogels in water. We hypothesized that covalent cross-linking of the NFC could even provide micro- and nanoscale shape-recovery properties by interlocking the fibrillar "struts" of the NFC aerogel.

As base nanocellulose material we used carboxymethylated NFC with approximate diameters of 2–3 nm and lengths of 2–3 μm. The NFC was produced by treating the sulfite-dissolving pulp of softwood with mono-chloroacetic acid (2 wt%) to introduce charged carboxylic groups (550 $\mu eq g^{-1}$), followed by mechanical disintegration with a homogenizer.[12] We further used 1,2,3,4-butanetetracarboxylic acid (BTCA) as a cross-linker, as BTCA is known to form

[*] Dr. M. Hamedi, E. Karabulut, A. Marais, Dr. G. Nyström, Prof. L. Wågberg
Department of Fibre and Polymer Technology, and Wallenberg Wood Science Centre, KTH Royal Institute of Technology
Teknikringen 56, 10044 Stockholm (Sweden)
E-mail: mahiar@kth.se
Dr. A. Herland
Department of Cell and Molecular Biology
Karolinska Institute, Solna (Sweden)

[**] We acknowledge funding from the Wallenberg Wood Science Centre, and from the Power paper project at Linköpings University, both funded by the Knut and Alice Wallenbergs (KAW) Research Foundation, and funding from BiMaC Innovation at KTH. We thank Koshi H for graphics production, Johanna Hornatowska for X-ray microtomography, and Innventia AB for providing the NFC material.

Supporting information for this article is available on the WWW under http://dx.doi.org/10.1002/anie.201305137.

ester linkages by reactions with cellulosic hydroxy groups.[14] The aerogels were made by dissolving powders of BTCA and sodium hypophosphite inside a NFC gel (2wt%), whereupon the gel was freeze-dried to achieve an aerogel. The aerogel was subsequently heated to 170°C, for initiating the covalent chemical reaction in the dry state, which resulted in a cross-linked aerogel (for details, see the Supporting Information). Aside from cross-linking, each BTCA molecule also adds two extra carboxyl groups to the aerogel; this results in an even higher total anionic surface charge, which is beneficial for the LbL preparation procedure. NFC aerogels with different degrees of cross-linking were characterized using IR spectroscopy and conductometric titrations. Figure 1c shows the

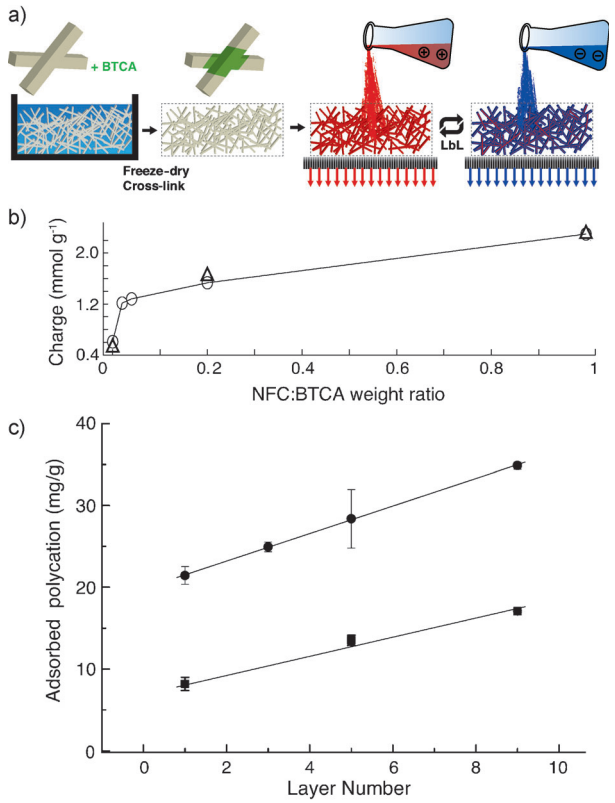

Figure 1. a) Representations of the cross-linking in NFC, and aerogel construction and the LbL assembly on aerogels. b) Conductometric charge (△), the charge calculated from the IR peak area around 1720 cm^{-1} and normalized with the conductometric charge (○). c) Adsorbed amount of PEI (●) and PAH (■) per gram of aerogel mass as a function of the total number of layers.

surface charge for the different degrees of cross-linking, which was measured conductometrically and can also be seen in the increasing area around the peak at 1720 cm^{-1} in the IR spectrum (Supporting Information, Figure S2). The maximum cross-linking increased the charge by 440% to 2300 μmol g^{-1}. This value is among the highest surface charge densities reported for aerogels, which makes this material ideal for a self-assembly procedure that is based on ionic surface interaction. Indeed, the average distances between the charges on the aerogel surface are smaller than the Bjerrum length in water at room temperature, and thus other factors, such as salt concentration and pH, will determine the available charge density[15] during the LbL assembly.

The cross-linked aerogels were further characterized mechanically in the wet state by compressive stress–strain measurements of aerogels immersed in water (Figure 3a). Here, the aerogels showed full and repeatable shape recovery up to a compressive strain of 95% in water, which still permitted total shape recovery down to the micro- to nanoscale when the pressure was released (Supporting Information, Figure S1). The compressive-stress values measured at the highest strains were greater than 1.6 MPa, which is one of the highest values ever reported for a compressible organic aerogel, and even exceeds values previously reported for CNT-based aerogels at recovery strain points.[16] Furthermore, these cross-linked aerogels are stable in most organic solvents, thus providing possibilities for non-aqueous LbL assembly or post-assembly functions in numerous liquids.

We hypothesized that a water-stable aerogel with a high specific surface charge would be a perfect material for a LbL assembly on the entire surface of the aerogel. However, as slow methods such as dip coating, or rapid LbL methods such as spray coating[17] only work for flat or macroporous surfaces,[9] we developed a LbL method that utilized the inherent properties of the strong aerogels by forcing solutions of polyelectrolytes through the aerogel by means of a pressure gradient (see the Supporting Information and Figure 1a). We found that the entire bulk of the aerogel surface could be covered in less than one second. The good surface coverage of each layer resulted in complete charge reversion of the surface, which allowed the consecutive growth of multiple numbers of layers. The success of this extremely rapid, yet high surface-area LbL coverage can be attributed to a combination of several factors. The time required to reach equilibrium adsorption probably decreases with increasing surface charge density, which was high in this case, especially at low salt concentrations.[18] The flow of liquid through a tortuous porous structure (Figure 2b,c; see also the Supporting Information, Movies S1 and S2) disrupts the linear flow and probably prevents the build-up of thick stagnant layers through which the polymers would have to diffuse. The amounts of adsorbed poly(ethyleneimine) (PEI) and poly(allylamine hydrochloride) (PAH), which were determined by nitrogen elemental analysis, are shown as a function of the number of layers in Figure 1c. Here, a smaller amount of PAH is adsorbed at the first layer as compared to PEI, and the adsorbed amounts of both materials show linear growth with increasing layers. These trends are similar to those for LbL growth on planar surfaces.[19] Using the adsorbed mass of the LbL layers, we roughly calculated a one-layer thickness of 0.3 nm for PAH, and 0.7 nm for PEI (see the Supporting Information). These numbers are close to values reported for planar LbL surfaces,[19] which indicates that the LbL coating should cover a large fraction of the specific surface area of the aerogel.

For LbL studies and the preparation of aerogels with several different functionalities, we used four different materials (Figure 2a); this included two water-soluble conducting polymers, sodium poly[2-(3-thienyl)ethoxy-4-butyl-

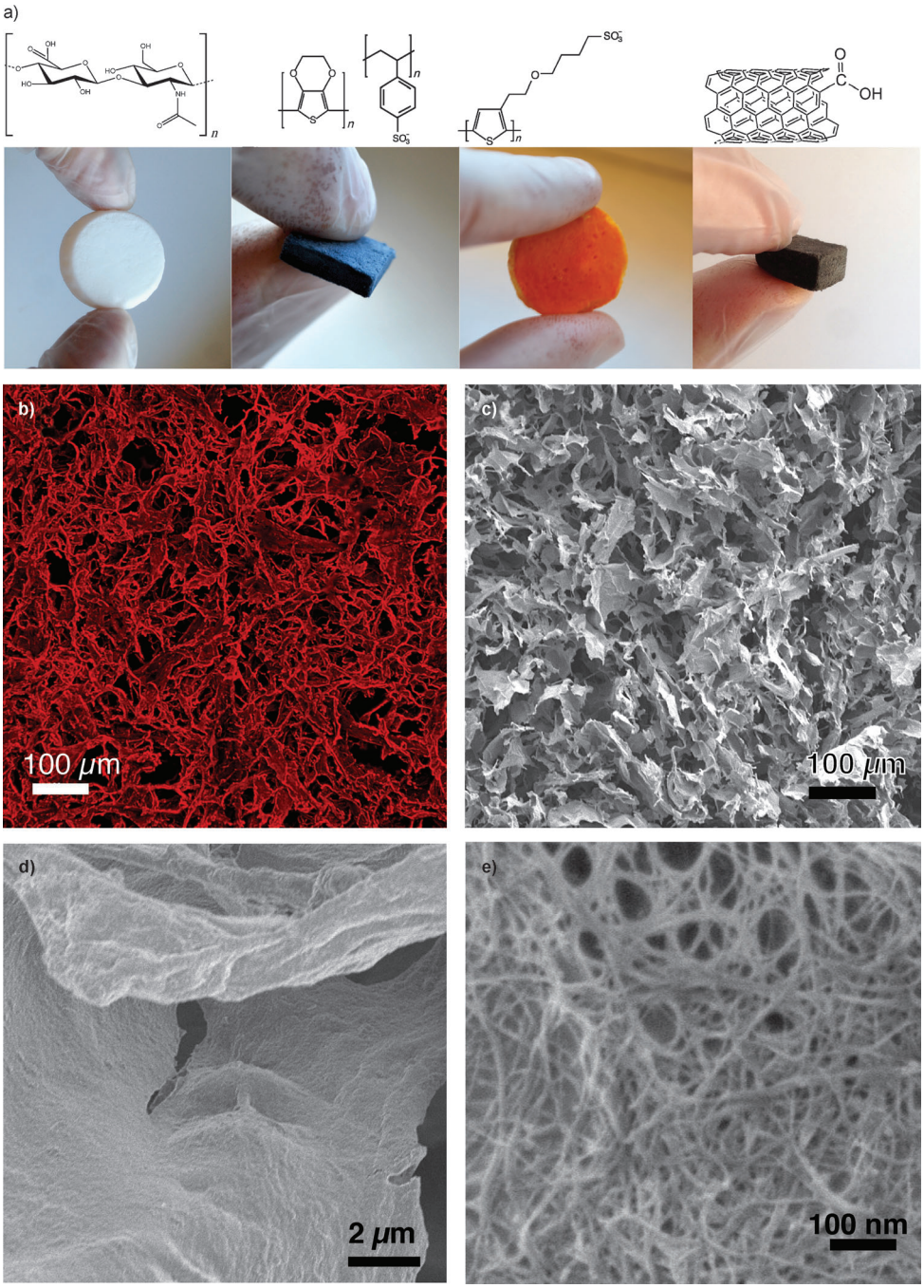

Figure 2. a) Optical micrographs of LbL-functionalized aerogels in the dry state, and the corresponding chemical formulas of the functional polyanion used in the LbL. Aerogel intersections were cut with a razor to display the interior part. The LbL coating from left to right shows: $(PAH/HA)_5$, $(PEI/PEDOT:PSS)_{10}$, $(PEI/ADS2000P)_{10}$, $(PEI/SWCNT)_5$. b) 3D picture reconstructed from slice images obtained by confocal microscopy from the fluorescence of LbL multilayers of $(PEI/ADS2000P)_{10}$ taken in dry state. SEM images are all taken at intersections inside coated aerogels, and show $(PEI/PEDOT:PSS)_{10}$ (c and d) and $(PEI/CNT)_5$ (e).

sulfonate] (ADS2000P), which is fluorescent and used here to study the three-dimensional structure of the LbL coating with confocal microscopy, and poly(3,4-ethylenedioxythiophene): poly(styrenesulfonate) (PEDOT:PSS), which is the most versatile of all conducting polymers. PEDOT-covered aerogels would open a door to a wide range of electronic, optoelectronic, and bioelectronic applications.[20] Furthermore, the biopolymer hyaluronic acid (HA), which has been widely used over the past few years in multilayer structures for biomedical applications, was tested.[21] Finally, single-wall carbon nanotubes (SWCNTs) were used for a LbL assembly of mesoscopic objects, which allow numerous possibilities[22] for electronic functionality of aerogels.

Micrographs and scanning electron microscopy (SEM) images were taken by cutting intersections into the aerogels. A uniform color of the coating revealed that the entire bulk of the aerogel was covered with materials assembled by LbL (Figure 2a). To study the bulk coating in more detail, we used confocal microscopy to image aerogels coated with ten bilayers of ADS2000P. A reconstructed image of the 3D structure of the fluorescent LbL layer is shown in Figure 2b and Movie S3, and reveals that the overall structure of the LbL coating extends into the aerogels with an overall uniform intensity, thus suggesting a uniform coverage of the aerogel surface. This confocal image can be compared to the SEM image (Figure 2c); both reveal the same microstructures and similar pore structures, and display the structures of the porous NFC nanofilms. Higher-magnification SEM images of aerogels coated with ten bilayers of PEI/PEDOT:PSS reveal an appearance very similar to that of pristine aerogels (Figure 2d), as the polymer coatings are only a few nanometers thick and quite uniform, which is a feature of successfully grown LbL films, where all residues have been washed between each LbL step to ensure growth and smoothness at the nanoscale. A SEM image of aerogels coated with five bilayers of PEI/SWCNT at a closer magnification is shown in Figure 2e. In contrast to the polymer LbL film, here the

structure of the LbL films is indeed visible, displaying a random network of SWCNT nanowires.

Compressive stress–strain experiments of a pristine aerogel and aerogels coated with ten layers of PAH/HA immersed in water showed very high compressibility and total shape recovery (Figure 3a). The PAH/HA-coated aerogels showed

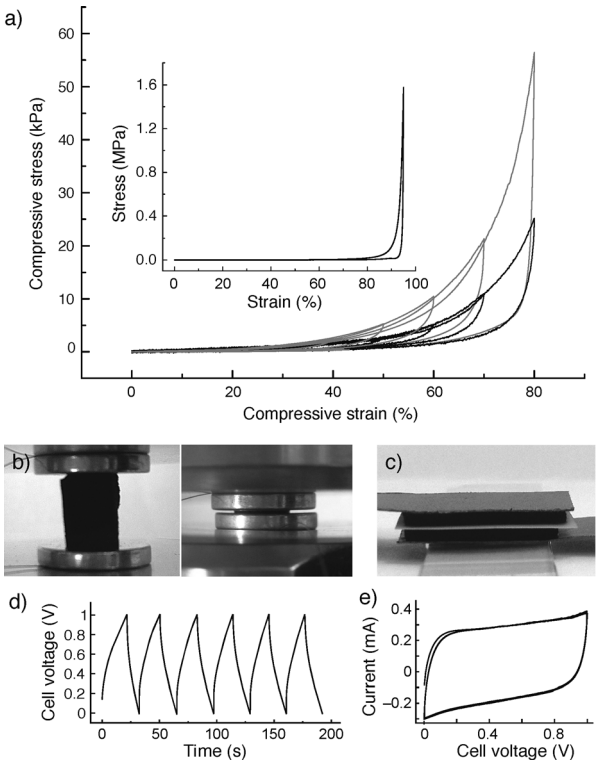

Figure 3. a) Reversible compressive strain vs. stress for aerogels in water, for a pristine aerogel (black) and for an aerogel with $(PAH/HA)_5$ (gray); inset: reversible compressive strain/stress up to 95% strain for $(PAH/HA)_5$. b) Photographs of a $(PEI/SWCNT)_5$ aerogel in the compression/resistance measurement setup in uncompressed and compressed state. c) Photograph of a supercapacitor device with two $(PEI/SWCNT)_5$ aerogels sandwiched with a spacer and connected to an anode and cathode graphite foil at top and bottom. d) Galvanostatic cycling. e) Cyclic voltamogram of the supercapacitor.

an increase of over 100% in compressive stress at all strains, with a retained increase in stress even at 80% strain. This is a considerable increase, especially considering that the LbL film is thin, and that the pristine aerogel already has one of the highest recovery stresses reported. The increase in strength can be attributed to the properties of the PAH/HA alloy formed through the LbL addition.[19] Further analysis of the mechanical properties of the aerogels in the dry state revealed that aerogels coated with five bilayers of PEI/SWCNT had a more pronounced elastic region up to 2% strain. They further showed a greater overall stress in the strain-hardening region, and were over three times stronger, with a stress of over 350 KPa. The large increase in mechanical strength indirectly revealed that the SWCNT coatings must have a high overall bulk coverage.

The aerogel with ten bilayers of PEI/PEDOT:PSS displayed high conductivity over large distances between electrodes, with a bulk conductivity of $1.4\times10^{-5}\,S\,cm^{-1}$. Values of around $10^{-3}\,S\,cm^{-1}$ have been reported[23] for similar LbL films on flat surfaces, so considering that the aerogel volume consists of about 98% air, our value suggests an almost complete LbL surface coverage. The resistance further decreased almost linearly with increasing strain, with a decrease of over 550% at 70% strain (Figure S4). The linearity suggests that the thin polymer film is flexible and conforms during the compression, while maintaining an almost constant thin-film conductivity even up to 70% strain.

For the uncompressed aerogel coated with five bilayers of PEI/SWCNT, a bulk conductivity of $1.2\times10^{-3}\,S\,cm^{-1}$ was measured. For planar LbL films of five bilayers of PEI/SWCNT, conductivities in the order of $10^{-2}\,S\,cm^{-1}$ [24] have been reported. Again, considering that the LbL film covers only a small weight percentage of the total bulk mass, our values not only suggest that we have a uniform coverage of CNT LbL, but also that we might have higher local film conductivities than those that were made using dip-coating on planar surfaces. The resistance of the SWCNT-coated aerogel displayed a more rapid decrease as a function of strain in the initial region up to 20% strain, and decreased by around 800% at 70% strain (Figure S4). We could also show a reversible change in resistance as a function of pressure within the elastic regime (Figure S4, inset), with a 30% decrease in resistance at a pressure of 14 KPa.

To show an active function that is based on the large available interfacial area between the LbL coating and a solution, we built an energy-storage device. Here, SWCNT-functionalized aerogels were used as electrodes in an aqueous supercapacitor (Figure 3c). This device showed almost perfect, square-shaped double-layer capacitive behavior in cyclic voltammetry (Figure 3e), and stable galvanostatic cycling over many cycles (Figure 3d). By accounting only for the measured weight of the active LbL layer, the specific electrode capacitance was calculated to be $419\pm17\,F\,g^{-1}$ (see the Supporting Information). This largely exceeds the best values previously reported for SWCNTs on paper substrates ($200\,F\,g^{-1}$),[25] SWCNT LbL freestanding films ($159\,F\,g^{-1}$),[26] and LbL multiwall-CNT films coated on carbon paper ($104\,F\,g^{-1}$).[8] The high specific capacitance found for these aerogel electrodes that were obtained by the LbL assembly of CNTs reflects the fact that the LbL method successfully provides an ultrathin nanoporous coating that maintains good connectivity throughout the whole aerogel-network structure. This in turn leads to improved use of the active material.

In conclusion, we have constructed aerogels with a high surface area and high surface charge, and demonstrated a rapid method for the LbL assembly of functional materials onto these aerogels. Conducting polymers, biomolecules, and carbon nanotubes were assembled by LbL, and enhanced compressive strength, super elasticity in the wet state, fluorescence, elastic mechanoresponsive resistance, and very high charge-storage capacity were observed. LbL-coated aerogels open avenues for functional mesoporous materials with many possibilities. Some application areas envisioned include aerospace,[27] energy storage,[8] thermoelectric materi-

als,[28] gas sensing,[29] biomedical devices,[21] drug delivery,[30] fire-resistant materials,[31] elastomeric aerogels,[32] and strong and superlight composites.[33,34]

Received: June 14, 2013
Revised: August 6, 2013
Published online: September 23, 2013

Keywords: aerogels · carbon nanotubes · layered compounds · mesoporous materials · nanocellulose

[1] S. M. Jung, H. Y. Jung, M. S. Dresselhaus, Y. J. Jung, J. Kong, *Sci. Rep.* **2012**, *2*, 849.
[2] M. Worsley, P. Pauzauskie, *J. Am. Chem. Soc.* **2010**, *132*, 14067 – 14069.
[3] Z.-S. Wu, S. Yang, Y. Sun, K. Parvez, X. Feng, K. Müllen, *J. Am. Chem. Soc.* **2012**, *134*, 9082 – 9085.
[4] M. Wang, I. V. Anoshkin, A. G. Nasibulin, J. T. Korhonen, J. Seitsonen, J. Pere, E. I. Kauppinen, R. H. A. Ras, O. Ikkala, *Adv. Mater.* **2013**, *25*, 2428 – 2432.
[5] R. T. Olsson, M. A. S. Azizi Samir, G. Salazar-Alvarez, L. Belova, V. Ström, L. A. Berglund, O. Ikkala, J. Nogués, U. W. Gedde, *Nat. Nanotechnol.* **2010**, *5*, 584 – 588.
[6] G. Decher, *Science* **1997**, *277*, 1232 – 1237.
[7] G. Decher, J. Schlenoff, *Multilayer Thin Films—Sequential Assembly of Nanocomposite Materials*, 2nd ed., Wiley-VCH, Weinheim, Germany, **2012**.
[8] S. Y. Kim, J. Hong, R. Kavian, S. W. Lee, M. N. Hyder, Y. Shao-Horn, P. T. Hammond, *Energy Environ. Sci.* **2013**, *6*, 888 – 897.
[9] Y. Kim, R. Harris, R. Davis, *ACS Macro Lett.* **2012**, *1*, 820 – 824.
[10] X. Roy, P. Sarazin, B. D. Favis, *Adv. Mater.* **2006**, *18*, 1015 – 1019.
[11] D. Klemm, F. Kramer, S. Moritz, T. Lindström, M. Ankerfors, D. Gray, A. Dorris, *Angew. Chem.* **2011**, *123*, 5550 – 5580; *Angew. Chem. Int. Ed.* **2011**, *50*, 5438 – 5466.
[12] L. Wågberg, G. Decher, M. Norgren, T. Lindström, M. Ankerfors, K. Axnäs, *Langmuir* **2008**, *24*, 784 – 795.
[13] W. Zhang, Y. Zhang, C. Lu, Y. Deng, *J. Mater. Chem.* **2012**, *22*, 11642.
[14] C. M. Welch, *Crosslinking Catal.* **1991**, 29 – 34.
[15] A. B. Fall, S. B. Lindström, O. Sundman, L. Ödberg, L. Wågberg, *Langmuir* **2011**, *27*, 11332 – 11338.
[16] K. H. Kim, Y. Oh, M. F. Islam, *Nat. Nanotechnol.* **2012**, *7*, 1 – 5.
[17] M. Lefort, G. Popa, E. Seyrek, R. Szamocki, O. Felix, J. Hemmerlé, L. Vidal, J.-C. Voegel, F. Boulmedais, G. Decher, et al., *Angew. Chem.* **2010**, *122*, 10308 – 10311; *Angew. Chem. Int. Ed.* **2010**, *49*, 10110 – 10113.
[18] M. A. Cohen Stuart, C. W. Hoogendam, A. de Keizer, *J. Phys. Condens. Matter* **1997**, *9*, 7767 – 7783.
[19] A. Marais, S. Utsel, E. Gustafsson, L. Wågberg, *Carbohydrate Polym.* **2013**, DOI: 10.1016/j.carbpol.2013.03.049.
[20] S. Kirchmeyer, K. Reuter, *J. Mater. Chem.* **2005**, *15*, 2077-2088.
[21] T. Boudou, T. Crouzier, K. Ren, G. Blin, C. Picart, *Adv. Mater.* **2010**, *22*, 441 – 467.
[22] M. F. L. De Volder, S. H. Tawfick, R. H. Baughman, A. J. Hart, *Science* **2013**, *339*, 535 – 539.
[23] R. Smith, A. Smith, J. Stricker, B. E. Taylor, M. F. Durstock, *Macromolecules* **2006**, *39*, 6071 – 6074.
[24] Y. Tian, J. G. Park, Q. Cheng, Z. Liang, C. Zhang, B. Wang, *Nanotechnology* **2009**, *20*, 335601.
[25] L. Hu, J. W. Choi, Y. Yang, S. Jeong, F. La Mantia, L.-F. Cui, Y. Cui, *Proc. Natl. Acad. Sci. USA* **2009**, *106*, 1 – 5.
[26] S. W. Lee, B. Kim, S. Chen, Y. Shao-horn, P. T. Hammond, *J. Am. Chem. Soc.* **2009**, *131*, 671 – 679.
[27] J. P. Randall, M. A. B. Meador, S. C. Jana, *ACS Appl. Mater. Interfaces* **2011**, *3*, 613 – 626.
[28] M. He, F. Qiu, Z. Lin, *Energy Environ. Sci.* **2013**, *17*, 14 – 17.
[29] Q. Ji, I. Honma, S.-M. Paek, M. Akada, J. P. Hill, A. Vinu, K. Ariga, *Angew. Chem.* **2010**, *122*, 9931 – 9933; *Angew. Chem. Int. Ed.* **2010**, *49*, 9737 – 9739.
[30] L. J. De Cock, S. De Koker, B. G. De Geest, J. Grooten, C. Vervaet, J. P. Remon, G. B. Sukhorukov, M. N. Antipina, *Angew. Chem.* **2010**, *122*, 7108 – 7127; *Angew. Chem. Int. Ed.* **2010**, *49*, 6954 – 6973.
[31] Z.-Y. Wu, C. Li, H.-W. Liang, J.-F. Chen, S.-H. Yu, *Angew. Chem.* **2013**, *125*, 2997 – 3001; *Angew. Chem. Int. Ed.* **2013**, *52*, 2925 – 2929.
[32] R. Gill, M. Mazhar, O. Félix, G. Decher, *Angew. Chem.* **2010**, *122*, 6252 – 6255; *Angew. Chem. Int. Ed.* **2010**, *49*, 6116 – 6119.
[33] A. A. Mamedov, N. A. Kotov, M. Prato, D. M. Guldi, J. P. Wicksted, A. Hirsch, *Nat. Mater.* **2002**, *1*, 190 – 194.
[34] P. Podsiadlo, M. Michel, K. Critchley, S. Srivastava, M. Qin, J. W. Lee, E. Verploegen, A. J. Hart, Y. Qi, N. A. Kotov, *Angew. Chem.* **2009**, *121*, 7207 – 7211; *Angew. Chem. Int. Ed.* **2009**, *48*, 7073 – 7077.